Hindawi Publishing Corporation
Journal of Spectroscopy
Volume 2015, Article ID 805649, 9 pages
http://dx.doi.org/10.1155/2015/805649

Research Article

SERS Characterization of the Indocyanine-Type Dye IR-820 on Gold and Silver Nanoparticles in the Near Infrared

Tatiana B. V. Neves and Gustavo F. S. Andrade

Laboratório de Nanoestruturas Plasmônicas, Núcleo de Espectroscopia e Estrutura Molecular, Departamento de Química, Universidade Federal de Juiz de Fora, Campus Universitário, Rua José Lourenço Kelmer s/n, 36036-900 Juiz de Fora, MG, Brazil

Correspondence should be addressed to Gustavo F. S. Andrade; gustavo.andrade@ufjf.edu.br

Received 14 October 2014; Revised 21 November 2014; Accepted 2 December 2014

Academic Editor: Nicolae Leopold

The Raman spectrum of the indocyanine-type dye IR-820 has been assigned for both solid and solution. SERS spectra of IR-820 on both silver and gold nanoparticles suspensions excited at 1064 nm were obtained. AgNPs allowed the detection of the dye through SERS down to 0.1 micromoles per liter; for the AuNPs the lowest concentration of the dye detectable was 10 micromoles per liter. Changes in the SERS relative intensities compared to the Raman spectrum in solution are subtle, mostly due to the preresonance effect of the dye. However, a perpendicular orientation relative to the metallic surface was inferred for the dye on both AgNPs and AuNPs. The easily distinguishable SERS spectra of the dye excited at 1064 nm, together with the high biological compatibility of cyanine dyes, are both indicative that IR-820 could be used as a high-performance probe molecule for SERS.

1. Introduction

The surface-enhanced Raman scattering (SERS) effect has been studied for almost 40 years [1–3]. The importance of the morphological properties of coinage metal nanostructures in providing large Raman signal amplification cannot be overestimated, as they are essential in the better understanding and development of the field. The SERS effect depends so strongly on the size, shape, and nature of metallic nanostructures that it has been tightly attached to nanoscience development over the past decades [4]. The strong dependence of the SERS enhancement on the geometrical properties of metallic nanostructures led to many studies that were focused on the optimization of nanostructures through different synthesizing methods. These methods could accurately control features such as the shape and the size of the metal nanoparticles [5]. The great effort put in the preparation of highly efficient SERS substrates resulted in the ability of applying the SERS effect in a wide range of fields, such as electrochemistry [6], advanced materials [7], environmental sciences [8], and biosensing [9], among other applications [10, 11]. Potential applications of the SERS effect as a bioanalysis technique have been strongly explored over the last few years [12]; such applications have actually been extended to *in vivo* applications in diagnostics [13, 14].

In addition to the dependence on the metallic nanoparticle characteristics, SERS is a strongly molecule and wavelength dependent effect, with the efficiency of the enhancement effect ranging over several orders of magnitude [15]. Approaches for the implementation of SERS in biological systems usually employ high-performance SERS-tags, which may include cyanine dyes, such as indocyanine [16]. Cyanine dyes usually present a very large Raman cross-section that might reach 7×10^{-25} cm^2 srad^{-1} in preresonance conditions for some merocyanines [17]. Single-molecule SERS detection has already been verified for the indocyanine green dye [16, 18].

The use of near-infrared (NIR) excitation in SERS studies of biological systems is of great importance, as it is usual to observe intense fluorescence background contributions from components of the system itself when the excitation occurs in the visible range of frequency. This being said, the use of FT-Raman is attractive for such measurements with excitations at 1064 nm. However, there have only been a small number of works reporting the use of excitation at 1064 nm for SERS [19, 20]. It is important to notice that the efficiency

of the local field localization decreases in the NIR, and the SERS enhancement factors may decrease greatly [21]. This drawback introduces the pressing necessity of combining high-performance SERS substrates with high-performance SERS probes. Recently, the emeraldine-form of polyaniline has been proposed as a high-performance SERS probe with excitation at 1064 nm [22]. As such, it would be interesting to have a more easily available probe molecule, which could be readily used in SERS experiments.

Taking into account the properties of cyanine-dyes, the IR-820 dye (structure presented in Scheme 1(a)) has been selected as a molecular probe for SERS with excitation in 1064 nm. The vibrational Raman and IR characterization of the IR-820 dye are also presented.

2. Experimental Section

All chemicals were purchased from Sigma-Aldrich and IR-820, $HAuCl_4$, $AgNO_3$, and sodium citrate were of high purity and were used without further purification. Deionized water (R = 18.2 MΩ·cm^{-1}) was used in the preparation of all solutions. Au nanoparticle suspensions (AuNPs) were prepared through a well-established methodology [23]. To prepare the gold suspension, a solution of $HAuCl_4$ (0.01%) was kept boiling under reflux and 500 μL of citrate solution (1%) was added. After a few seconds the color changed to red. The silver nanoparticles (AgNPs) suspension has also been prepared using a well-known method [24]: in short, a solution of $AgNO_3$ (1.8 mmol L^{-1}) was kept boiling under reflux and a 1% citrate solution (2 mL) was added in the mixture; the resulting solution turned gray and it was kept boiling for ca. 1 hour. Both Au and Ag nanoparticle solutions were stored at 4°C before measurements.

UV-visible spectra were acquired with a Shimadzu UVPC1000 spectrometer, using a 10 mm fused silica cell. The FTIR spectrum was acquired from the solid IR-820 dispersed in KBr pellet with a Bomem MB100 spectrometer. The Raman spectra have been acquired with a Bruker RFS 100 spectrometer and a Nd^{3+}/YAG laser with a line at 1064 nm and with a 4 cm^{-1} spectral resolution, equipped with a Ge detector cooled with liquid nitrogen. The SERS spectra were acquired using different concentrations of IR-820: 0.1, 1.0, 10.0, and 100 μmol L^{-1} in both gold and silver suspensions using a 300 mW laser power and 200 scans; the AgNPs and AuNPs suspensions were diluted 5 times using deionized water for the SERS experiment and, before the addition of the dye, a final concentration of 43 mmol L^{-1} KCl was added to the nanoparticle suspensions, in order to trigger the aggregation of the nanoparticles and improve the SERS performance [25]. Raman spectra of the liquid state were also obtained using 200 scans and a 300 mW laser power.

The structure and vibrational frequencies of IR-820 have been calculated using the Gaussian09 suite of programs [26] at DFT level of theory, using the hybrid functional B3LYP [27–29], and the triple-ζ basis function set 6-311G(d,p) [30, 31]. The geometry optimization was performed without any constraint; there has been no calculated imaginary frequency, confirming that the calculated structure corresponds to a local-minimum of the potential energy surface. The calculated Raman activity has been converted to calculated Raman intensity by a correction for the scattering frequency (considering excitation at 1064 nm) and assuming a finite temperature of the sample (considered to be 25°C) [32]. Calculated Raman and infrared spectra were plotted from GaussView software [33] outputs considering a resolution of 4 cm^{-1}. No correction to the calculated vibrational wavenumbers has been used. The assignment of the vibrational bands has been made by visual inspection of the calculated vibrational modes. The atom numbering for the optimized IR-820 geometry (presented in Scheme 1(b)) and the z-matrix of the optimized structure in the B3LYP/6-311G(d,p) DFT calculations is available from the authors upon request. The molecular electrostatic potential (MEP) maps, presented in Scheme 1(c), have been plotted using GaussView.

3. Results and Discussion

The UV-VIS spectrum of an aqueous solution of IR-820 is presented in Figure 1. IR-820 is a cyanine dye that presents a strong and broad absorption band at 690 nm in aqueous solution, which has a molar absorptivity of 7.2 × 10^4 dm^3 mol^{-1} cm^{-1}, with a shoulder at ca. 819 nm. The shoulder at 819 nm is a hot-band, as it has been shown by acquiring the UV-VIS spectrum of an IR-820 solution at different temperatures. It should be noted that the broad absorption of IR-820 indicates that this dye might be in preresonance with the laser line at 1064 nm, used in the SERS measurements in the present work. Additionally, the absorption band at higher wavelengths in the UV-VIS spectrum of IR-820 has already been observed in other cyanine dyes. This band has been assigned to a charge transfer transition [34, 35].

3.1. Vibrational Assignment of the Raman and Infrared Spectra of IR-820. The potential use of IR-820 as a high-performance SERS probe requires an assignment of the Raman and infrared spectra of the dye. The Raman and infrared spectra of solid IR-820 are presented in Figure 2. The most intense bands in the spectra are marked in Figure 2, and a more extensive band position and vibrational assignment are presented in Table 1. This vibrational assignment has been performed taking into consideration the calculated Raman and infrared spectra of IR-820 in vacuum (presented in Figure 3) and references from experimental vibrational assignments [36]. In order to ensure clarity in the following discussion, the band assignment has been referred to calculated frequency values.

Table 1 shows that the low wavenumber bands at 308, 359, 392, and 461 cm^{-1} are assigned to out-of-plane CCC bending of the alkyl chain of the dye. Vibrational modes related to the CC stretching vibrations are assigned to the bands at 802 and 1072 cm^{-1}. The CH_2 bending vibrations have been assigned at 741, 768, and 1072 cm^{-1} for the rocking vibrations and 1174 and 1375 cm^{-1} for the twisting vibrations, wagging at 1392 cm^{-1} and CH_2 scissoring mode assigned to the band at 1504 cm^{-1}. The umbrella bending of CH_3 groups has been assigned at 1504 cm^{-1}, mechanically coupled to the CH_2 scissoring.

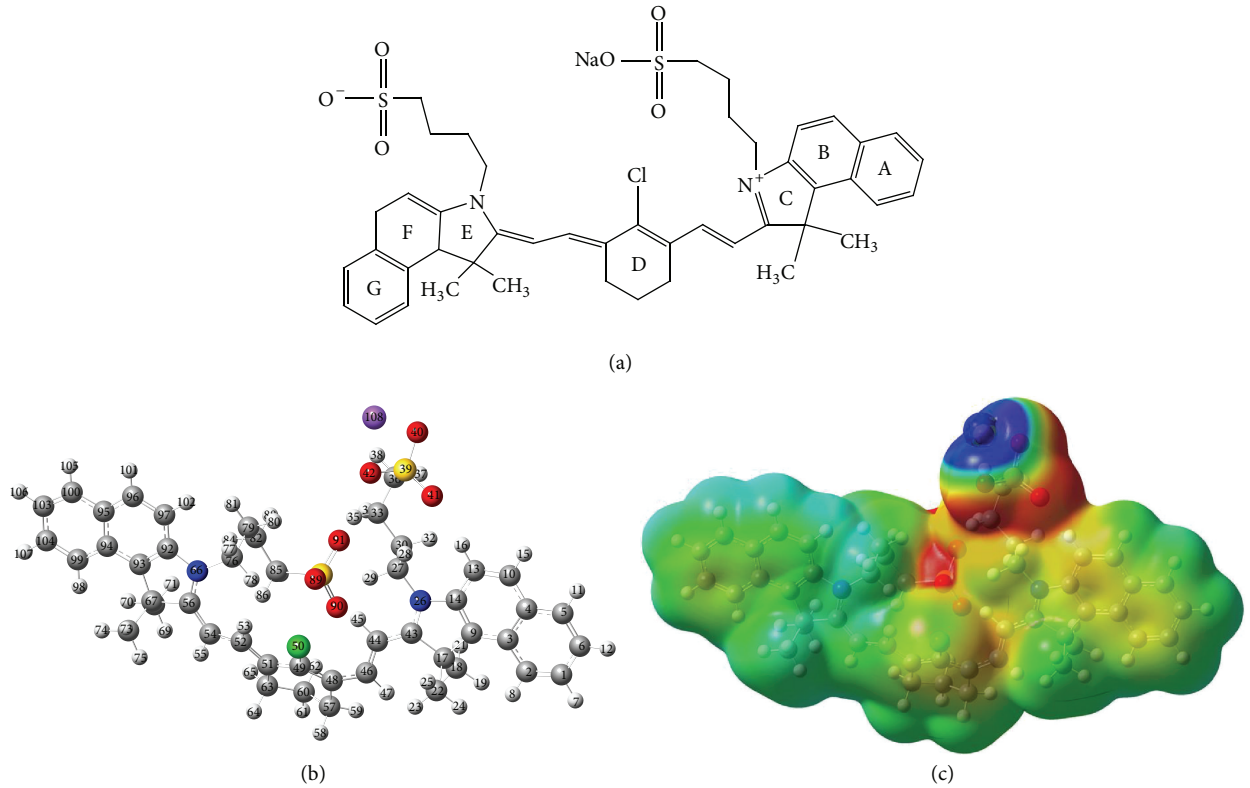

Scheme 1: (a) Schematic chemical structure of IR-820; the rings are labeled A–G. (b) Schematic structure of IR-820 optimized using DFT with the hybrid functional B3LYP and 6-311G(d,p) basis-set. The grey spheres represent C, blue for N, red for O, yellow for S, green for Cl, and purple for Na. (c) MEP maps for IR-820 calculated at the same level of theory as for (b); red-to-blue color scheme indicates negative-to-positive partial charges.

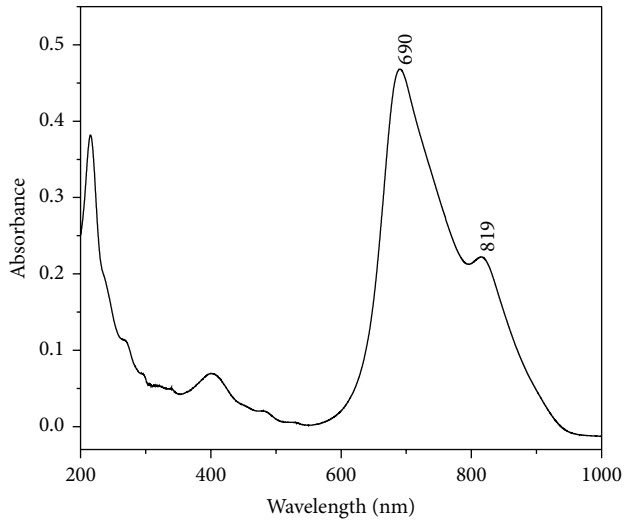

Figure 1: UV-VIS spectrum of an aqueous solution of 10 μmol L^{-1} IR-820.

The CCC bending of the conjugated central chain of IR-820 (see Scheme 1) has been assigned to the bands at 654 and 874 cm^{-1} and has also been found to contribute as a minor vibration in the mode assigned to the band at 392 cm^{-1}, which has been assigned above to the alkyl chain out-of-plane CCC bending. The stretching CC vibrations of the conjugated chain have been assigned to the bands at 1223, 1463, 1573, and 1603 cm^{-1}. The modes assigned to the 1463 and 1503 cm^{-1} band also have an important contribution from ν(CN); the CH bending of the same chain also contributes to the band at 1463 cm^{-1}. The δ(CH) vibration is also assigned to bands at 815, 943, 1274, 1375, 1382, and 1463 cm^{-1}. Additionally, a mode with predominant ν(CN) has been assigned to the band at 1392 cm^{-1}.

The modes that present contributions from different rings of the IR-820 dye have been each labelled by letters from A to G in Table 1, which may be found in the IR-820 structure in Scheme 1. The discussion of the assignment will be made without distinguishing between the rings. The ring CCC bending modes are assigned to the bands at 520, 595, 639, 654, 840, 874, and 911 cm^{-1}. The mode assigned to the band at 911 cm^{-1} also has a contribution from CH_2 twisting of ring D; additionally, the CH_2 rocking of ring D is assigned to the band at 815 cm^{-1}. The out-of-plane CH bending of the aromatic ring was assigned to the band at 718 cm^{-1}, and the in-plane CH bending can be assigned to bands at 1161, 1174, 1208, 1236, and 1482 cm^{-1}. The CC stretching modes have been assigned to the bands at 1011, 1046, 1072, 1562, 1640, and 1666 cm^{-1}.

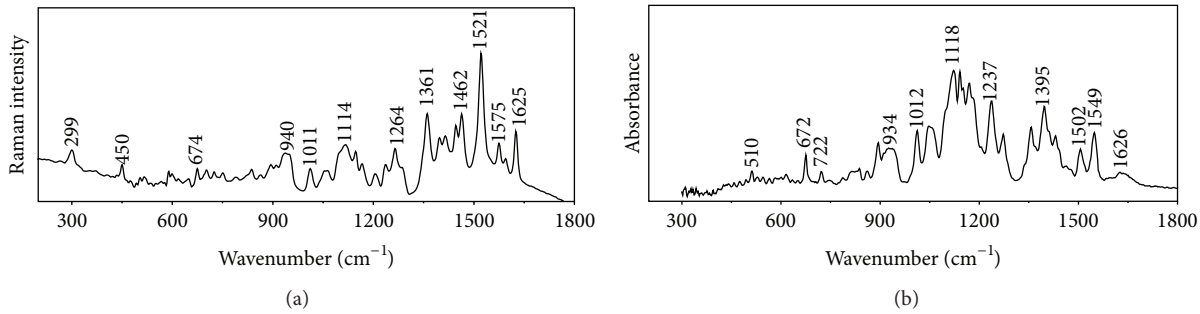

Figure 2: Experimental spectra of solid IR-820: (a) FT-Raman and (b) FTIR spectra.

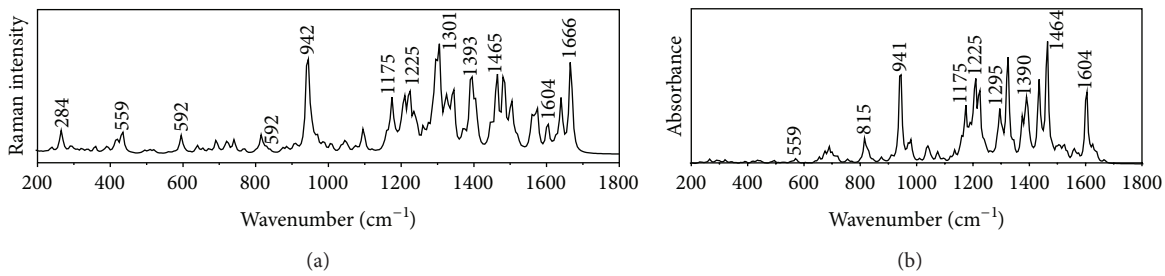

Figure 3: DFT calculated spectra of IR-820: (a) Raman and (b) infrared.

Finally, the band at 481 cm^{-1} has been assigned to the symmetric bending of the SO_3^- group and to the CS stretching (experimental at 503 cm^{-1}). On the other hand, the C-S stretching vibration is the dominant vibration at 691 cm^{-1}, and the SO stretching is assigned to the band at 1208 cm^{-1}.

3.2. SERS Spectra of IR-820 on Silver and Gold Nanoparticles. Figures 4(a) and 4(b) present the SERS spectra of the IR-820 dye on AuNPs and AgNPs, respectively, compared to the Raman spectra of a 100 μmol L^{-1} IR-820 solution. As it was expected, there is a considerable improvement in the signal-to-noise ratio as well as in the Raman intensity for both nanoparticle systems. It can also be observed that the SERS intensity is higher for IR-820 adsorbed on AgNPs, which resulted in SERS spectra for concentrations as low as 0.1 μmol L^{-1} of the dye. The difference in SERS intensity between AgNPs and AuNPs may be ascribed to the much larger size distribution obtained for the AgNPs compared to the AuNPs, through the preparation procedures used. As one can notice in the extinction spectra of both nanoparticles suspensions, presented in Figure 4(c), the FWHM for the band at 438 nm in the AgNPs spectrum is 160 nm, considerably larger than the FWHM = 108 nm in the AuNPs spectrum. This result indicates that the size distribution in AgNPs is larger than for AuNPs. Additionally, the presence of chloride results in a greater amount of aggregation for AgNPs than for AuNPs.

The SERS spectral profile of IR-820 on both AgNPs and AuNPs is somewhat similar to that reported for the indocyanine green (ICG) dye [16], which has already been reported as a high-performance molecular probe for SERS experiments. The most intense bands in the 1000–1600 cm^{-1} range of the SERS spectra are present in both spectra with similar wavenumbers and relative intensity. A very strong band at 1122 cm^{-1}, assigned to CH in-plane bending of the aromatic ring, is one of the most intense bands in the IR-820 SERS spectra, as well as in the ICG spectrum. Similar conclusions may be drawn for several very strong bands in the IR-820 SERS spectra, such as those at 943, 1207, 1440, and 1522 cm^{-1}, which are also very strong in the SERS spectra of ICG.

The SERS spectra of IR-820 on both AgNPs and AuNPs have also been compared to the Raman spectra of the dye in solution, also presented in Figure 4. One can observe that the relative intensity of bands assigned to different groups presented only subtle changes in the spectra of the adsorbed dye compared to the solution; all the compared bands could be observed in both spectra, and there have not been any noteworthy wavenumber changes. The lack of observable changes resulted in a simple band assignment for the SERS results, as it is being presented in Table 1, together with the Raman and FTIR spectra assignments. In spite of the similarities in the SERS and Raman spectra of IR-820, one can also observe that several relative intensities have changed. The most important observed changes have been noticed mostly in the low wavenumber region of the spectra.

Compared to the Raman spectra of IR-820 in solution, the bands at 450 and 1580 cm^{-1} present an increase in the relative intensity in the SERS spectra. Several other bands present changes in the relative intensity of the SERS spectra, taking the band at 1522 cm^{-1} as an example. It can also be observed that, for the bands at 943 and 1121 cm^{-1}, no shoulder or low intensity band is found in the SERS spectra, unlike what has been observed in the Raman spectrum in solution. In addition, the relative intensities of the bands at 943, 1121,

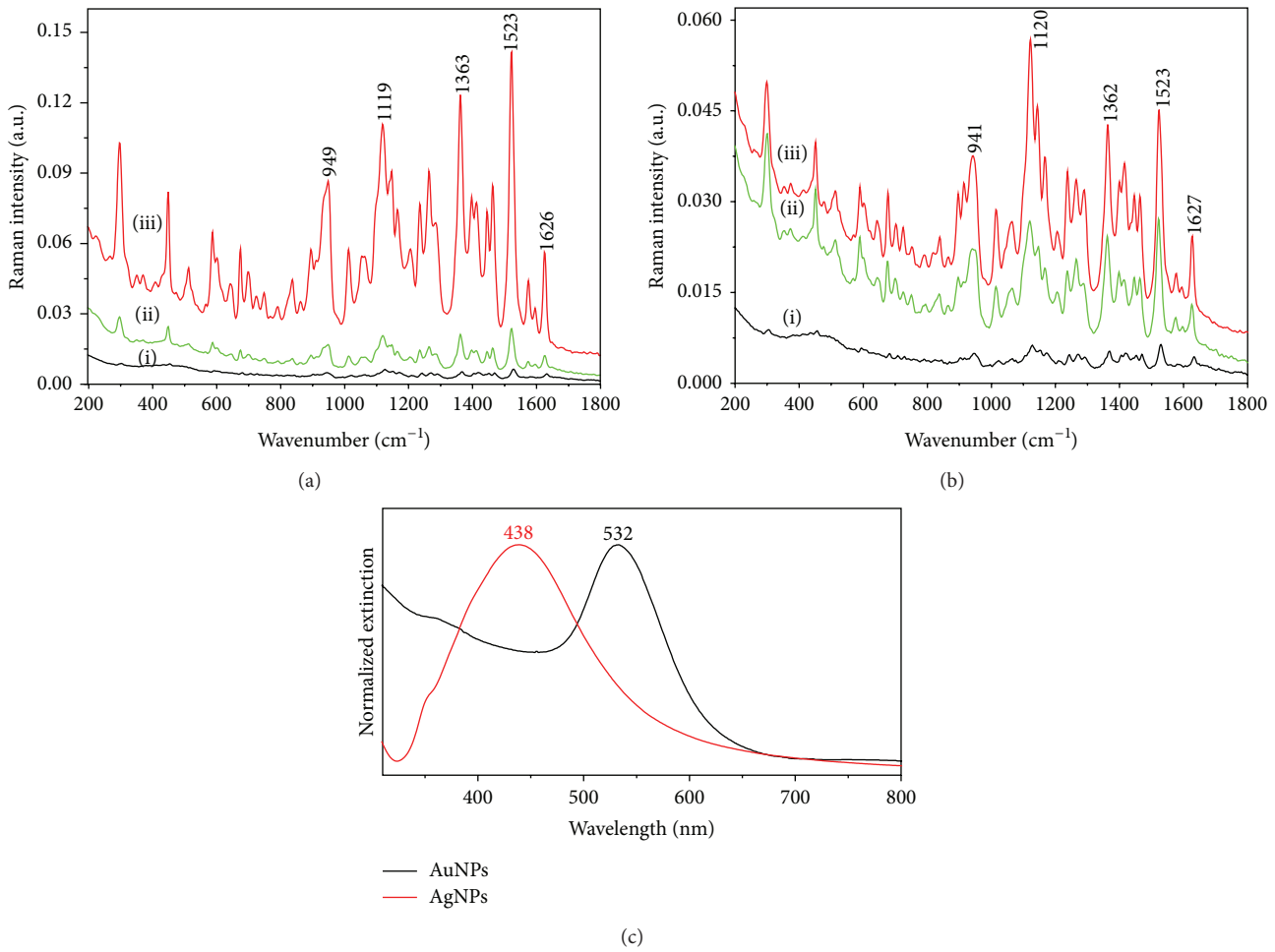

FIGURE 4: SERS spectra of IR-820 (a) at two solution concentrations on AgNP: (ii) 1 μmol L^{-1} and (iii) 0.1 μmol L^{-1}, compared to the Raman spectrum of the dye at 100 μmol L^{-1}; (b) at two solution concentrations on AuNP: (ii) 100 μmol L^{-1} and (iii) 10 μmol L^{-1}, compared to the Raman spectrum of the dye at 100 μmol L^{-1}. The spectrum labeled (i) in both items is the Raman spectrum of 100 μmol L^{-1} IR-820. (c) Extinction spectrum of the AuNPs and AgNPs used as SERS substrates.

and 1522 cm^{-1} changed considerably in the SERS spectra. The observation of the mentioned changes in SERS relative intensity results in a dependence of the SERS enhancement factor for IR-820 on the vibrational mode, as it will be discussed later in this work.

The changes in the SERS spectra compared to the Raman spectra are small, as has been demonstrated above. Although not conclusive, this result is indicative of a small contribution of the chemical mechanisms for the SERS effect in the case of IR-820 [4]. Due to the small number of adsorption centers for the dye, mostly amines that are heavily spatially hindered, it is actually not expected that the chemical interaction of the dye with the surface is strong. On the other hand, the dye and the surface stabilizer (citrate) are negatively charged, and IR-820 is observed in a zwitterionic form, such that it could be reasonable to expect an important electrostatic interaction between the dye and the metallic surfaces. Such a preferential interaction of groups of the IR-820 molecule with the surface could result in changes in the relative intensities in the SERS spectrum. If one compares the MEP results in Scheme 1(c) to the above discussion, an interesting correlation may be found. The MEP in Scheme 1(c) indicates a large accumulation of negative charges by the sulfonate groups, and some in the ring moieties, which is in a good correlation with the adsorption configuration proposed below on the basis of SERS relative intensities.

However, there are not many changes between the spectra of IR-820 in solution and the SERS relative intensities, which could be a result of the frequency proximity of the IR-820 absorption band at 690 nm (ε = 7.2 × 10^4 dm^3 mol^{-1} cm^{-1}) with a strong shoulder at 819 nm to the exciting radiation at 1064 nm (the difference in energy is 2800 cm^{-1}); such a proximity could indicate a preresonance of the FT-Raman exciting radiation with the lower energy electronic band of IR-820. It has been demonstrated that a preresonance condition in SERS experiments usually decreases the spectral changes with adsorption [37]. This characteristic is indeed observed in the SERS spectra of IR-820 excited at 1064 nm presented in Figure 4.

Table 1: Band wavenumber (in cm^{-1}) assignment for Raman, SERS (on Au and Ag nanoparticles), and infrared spectra of IR-820. λ_0 = 1064 nm.

Theoretical/cm^{-1}	Infrared/cm^{-1}	Raman solid/cm^{-1}	Raman solution/cm^{-1}	SERS (Ag)/cm^{-1}	SERS (Au)/cm^{-1}	Assignment*,**
308	—	299	300	300	298	$\delta(CCC)_{alk,oop}$
359	—	—	353	353	351	$\delta(CCC)_{alk,oop}$
392	—	—	371	374	370	$\delta(CCC)_{alk,oop} + \delta(CCC)_{conj}$
461	462	450	449	451	452	$\delta(CCC)_{alk,oop}$
481	510	503	474	476	478	$\delta(SO_3^-)_{sim} + \nu(CS)$
520	—	515	515	514	511	$\delta(CCC)_{F,G}$
595	—	588	—	590	589	$\delta(CCC)_{A,B,C}$
639	618	—	—	—	—	$\delta(CCC)_{A,B,C}$
654	—	—	646	647	645	$\delta(CCC)_{rings} + \delta(CCC)_{conj}$
691	672	674	675	675	676	$\nu(CS)$
718	—	702	701	701	699	$\delta(CH)_{rings,oop}$
741	722	725	725	726	724	$\delta(CH_2)_{r,alk}$
768	—	751	751	751	751	$\delta(CH_2)_{r,alk}$
802	786	790	789	792	790	$\nu(CC)_{alk}$
815	811	811	—	—	—	$\delta(CH)_{conj,oop} + \delta(CH_2)_{r,D}$
840	837	837	837	838	837	$\delta(CCC)_{E,F,G}$
874	860	862	863	863	863	$\delta(CCC)_{E,F,G} + \delta(CCC)_{conj}$
911	893	894	897	897	897	$\delta(CCC)_{A,B,C} + \delta(CH_2)_{t,D}$
943	934	940	940	944	941	$\delta(CH)_{conj,oop}$
1011	1012	1011	1016	1014	1015	$\nu(CC)_D$
1046	1051	1059	—	1054	—	$\nu(CC)_A$
1072	—	—	1064	1067	1063	$\delta(CH_2)_{r,alk} + \nu(CC)_D$
1161	1118	1114	1122	1122	1122	$\delta(CH)_{A,B,F,G}$
1174	1141	1146	1147	1148	1144	$\delta(CH)_{rings}$
1208	1171	1166	1171	1167	1169	$\delta(CH)_{A,B,F,G} + \delta(CH_2)_{t,alk,D} + \nu(SO)$
1223	—	1205	1209	1207	1205	$\nu(CC)_{conj}$
1236	1237	1235	1238	1235	1236	$\delta(CH)_{A,B,F,G}$
1274	1273	1264	1265	1265	1263	$\delta(CH)_{conj} + \delta(CH_2)_{t,D}$
1375	1375	1361	1361	1364	1363	$\delta(CH_2)_{t,alk} + \delta(CH)_{conj}$
1392	1392	1397	1399	1398	1400	$\delta(CH)_{conj} + \delta(CH_2)_{w,alk} + \nu(CN)$
1463	—	—	1415	1414	1415	$\delta(CH)_{conj} + \nu(CC)_{conj}$
1482	1446	1446	1447	1445	1446	$\delta(CH)_{rings}$
1504	1463	1462	1464	1465	1463	$\delta(CH_2)_{sc,alk} + \delta(CH_3)_{u,alk}$
1562	1523	1521	1522	1522	1523	$\nu(CC)_{A,B}$
1573	1549	—	—	—	—	$\nu(CC, CN)_{conj}$
1603		1575	1576	1575	1574	$\nu(CC)_{conj}$
1640	—	1595	1595	1596	1596	$\nu(CC)_{F,G}$
1666	1626	1625	1626	1625	1626	$\nu(CC)_{A,B}$

*ν: stretching; δ: bending; u: umbrella; sc: scissoring; t: twisting; r: rocking; w: wagging; conj: conjugated chain; alk: alkyl chain; A, B, C, D, E, F, and G: rings, referred to in Figure 2; oop: out-of-plane. **Assignment based on the visual inspection of vibrational eigenvectors calculated by DFT [B3LYP/6-311G(d,p)] and compared to the assignments from [36].

One interesting point resulting from the above characteristic of the SERS spectrum is that it is possible to directly calculate enhancement factors for IR-820 using the Raman spectrum as a reference, as the adsorbed chemical species is very similar to the solution species.

In order to evaluate the SERS spectra of IR-820 it is important to calculate the SERS enhancement factor (SERS-EF). Several methodologies for the SERS-EF calculation have been reported in the literature each of them being adequate for different types of SERS substrates and levels of knowledge

of surface behavior of the adsorbate [38]. Considering that there is a complete lack of experimental information on the adsorption behavior of the IR-820 dye, the characterization of the dye has been made on AgNPs and AuNPs in suspension. As such, the most used methodology for the calculation of SERS-EF, referred to as analytical enhancement-factor (AEF), has been chosen, as shown in the following equation [38]:

$$\mathrm{AEF} = \frac{I_{\mathrm{SERS}}/c_{\mathrm{SERS}}}{I_{\mathrm{Raman}}/c_{\mathrm{Raman}}}, \quad (1)$$

where I_{SERS} and I_{Raman} are the experimental SERS and Raman intensities, respectively, and c_{SERS} and c_{Raman} are the dye solution molar concentrations used in SERS and Raman experiments, respectively.

It should be noted that (1) assumes a model for the SERS enhancement that considers all molecules in the excited volume to present the same contribution to the SERS enhancement [38, 39]. For concentrations well above what is needed in order to fully cover the nanoparticles with a layer of the dye, the amount of adsorbate that is not in direct contact with the surface may be important. If a large number of molecules is not in contact with the nanoparticles surface and is not close enough to the surface to be under the influence of the enhanced local field of the metallic nanoparticles, it could strongly influence the SERS-EF calculations. The calculated SERS-EF of IR-820 on both AgNPs and AuNPs excited at 1064 nm for three different SERS bands and different concentrations are presented in Table 2. Comparing the SERS-EF of IR-820 adsorbed on AuNPs to the one of IR-820 adsorbed on AgNPs in concentrations of 10 μmol L^{-1}, it is easily observed that the enhancement factor of Ag is ca. 4.5 times larger than that of Au. Although the LSPR band of the AuNPs is closer to the Nd/YAG laser line, the larger AEF for silver may be better understood if one takes into consideration the fact that the size distribution in the AgNPs suspension is much broader than for AuNPs in the experimental conditions used [24]. The broader size distribution would indicate the possibility of obtaining large AgNPs in suspension, even in small concentrations, resulting in a better SERS performance. Additionally, in order to obtain the best possible SERS signal, 10 mmol L^{-1} KCl has been added to the solution for both nanoparticle suspensions; the amount of Cl^- added is known to considerably improve the SERS performance of the nanoparticle suspensions by inducing aggregation [25]. The Cl^- induced aggregation is much more effective in AgNPs due to specific interactions between Ag and Cl^-. If no KCl is added to the nanoparticle suspensions, SERS performances for both AgNPs and AuNPs are considerably lowered, which is strong evidence that the aggregation has a very important role in the performance of AgNPs and AuNPs suspensions as substrates for IR-820 SERS.

Another important observation from Table 2 is that the calculated SERS AEF strongly depends on the dye concentration for both AgNPs and AuNPs. For example, it can change from 1 to 3 orders of magnitude for AgNPs when changing concentrations from 100 to 0.1 μmol L^{-1}. This result is to be expected as a consequence of the simplicity of the AEF calculation, as discussed above [39]. This low accuracy occurs because the SERS intensity decreases strongly for molecules that are not in direct contact with the nanoparticle surface. It is worth noting that the monolayer saturation for smaller cyanine dyes, compared to IR-820, on silver halides occurs at the 1-2 μmol L^{-1} in aqueous media [40]. So, for concentration as high as 100 μmol L^{-1}, it is expected that a large portion of the molecules present in the AgNPs and AuNPs suspensions are not directly adsorbed on the surface of nanoparticles, thus contributing very little to the SERS enhancement.

Table 2: Analytical SERS-EF (AEF) for different concentrations of IR-820 on AgNPs and AuNPs calculated for three different bands. λ_0 = 1064 nm.

Metal	IR-820 concentration (μmol L^{-1})	SERS wavenumber (cm^{-1})	AEF
Ag	100	944	33
		1122	23
		1522	30
	10	944	271
		1122	173
		1522	257
	1	944	2764
		1122	1809
		1522	2810
	0.1	944	4270
		1122	2915
		1522	4013
Au	100	941	11
		1122	9
		1523	9
	10	941	63
		1122	39
		1523	86

The effect that the concentration of the adsorbate has on the SERS-EF decreases as the bulk concentration decreases, which results in an increase of the SERS-EF calculated with the AEF methodology [39]. It should be mentioned that the AEF model focuses mostly on the nature of the adsorbate, as there are no considerations about specific substrate properties. The focus on the substrate could be achieved by using different models for the calculation of SERS-EF [21]. The present work, however, is focused on the properties of the adsorbed IR-820 dye and not on the substrate. With this focus the AEF model for calculating the SERS-EF shows that the dye presents a strong SERS intensity when excited at 1064 nm. This is unusual, if SERS experiments on other dyes are taken into consideration, due to the decrease in the efficiency of the field localization by plasmonic resonances [21]. As a result, it has been possible to detect the dye in 0.1 μmol L^{-1}, which makes it an interesting candidate as a SERS probe molecule for excitations in the near infrared.

Figure 5 presents the SERS spectra of IR-820 compared to the SERS spectra of Rhodamine-6G (R6G), probably the most

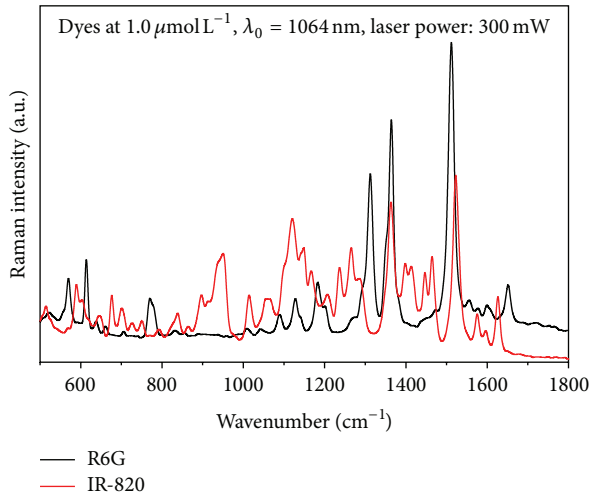

Figure 5: SERS spectra of 1.0 μmol L^{-1} solutions of IR-820 and R6G on AgNP under the same experimental conditions, for the comparison of relative SERS performances.

studied SERS dye, under the same experimental conditions and at a 1.0 μmol L^{-1} concentration. Figure 5 shows that Rhodamine-6G presented SERS intensities similar to IR-820.

The SERS-EFs also present a slight dependence on the vibrational mode, as it can be observed from the changes in the AEF calculated for the bands at 943, 1121, and 1522 cm^{-1} in Table 2. The AEF for the band at 1121 cm^{-1} is 30–38% lower than for the other two bands in all cases, except for the IR-820 concentration of 100 μmol L^{-1} on AuNPs. The three bands have been assigned to in-plane vibrational modes of the aromatic rings and the delocalized chain in the center of the structure of the dye (see Table 1); this result suggests that there is a preferential orientation of the dye molecule with the aromatic rings perpendicular to the metallic surface [41]. The changes in the IR-820 SERS intensities compared to the Raman spectrum in solution are subtle unlike several other molecules in the literature [42]. The small changes may be attributed to the preresonance condition of the dye for excitation at 1064 nm. The preresonance condition is thought to decrease the influence of orientation in the SERS relative intensities, which could explain the behavior of IR-820 in the present work [37].

4. Conclusion

The indocyanine-type dye IR-820 had the vibrational Raman and FTIR spectra assigned with the support of DFT calculations. The vibrational assignment was used in order to better understand the SERS spectra of the dye on AgNPs and AuNPs suspensions. The SERS relative intensities only presented small changes when compared to the Raman spectra of the dye in solution. Additionally, the SERS relative intensities presented a weak dependence on both the surface material and vibrational mode, which indicated weak surface interaction. The weak dependence of SERS relative intensities on the vibrational modes, however, indicated that the dye was adsorbed with the aromatic rings perpendicular to the surface.

The weak dependence of the SERS relative intensities on the metallic surface and on the vibrational modes indicates that IR-820 is an interesting candidate as a probe molecule for SERS with excitation in the near infrared. The ubiquitous use of FT-Raman spectroscopy also indicates that IR-820 may be an interesting probe for SERS on such configurations.

Conflict of Interests

The authors declare that there is no conflict of interests regarding the publication of this paper.

Acknowledgments

The authors thank FAPEMIG, CNPq, UFJF, and "Rede Mineira de Química" (RQ-MG-FAPEMIG) for financial support. Gustavo F. S. Andrade thanks CNPq for a research fellowship. Tatiana B. V. Neves thanks CAPES for the grant of a fellowship.

References

[1] M. Fleischmann, P. J. Hendra, and A. J. McQuillan, "Raman spectra of pyridine adsorbed at a silver electrode," *Chemical Physics Letters*, vol. 26, no. 2, pp. 163–166, 1974.

[2] D. L. Jeanmaire and R. P. van Duyne, "Surface Raman spectroelectrochemistry Part I. Heterocyclic, aromatic, and aliphatic amines adsorbed on the anodized silver electrode," *Journal of Electroanalytical Chemistry*, vol. 84, no. 1, pp. 1–20, 1977.

[3] M. G. Albrecht and J. A. Creighton, "Anomalously intense Raman spectra of pyridine at a silver electrode," *Journal of the American Chemical Society*, vol. 99, no. 15, pp. 5215–5217, 1977.

[4] M. Moskovits, "Surface-enhanced Raman spectroscopy: a brief retrospective," *Journal of Raman Spectroscopy*, vol. 36, no. 6-7, pp. 485–496, 2005.

[5] M. Fan, G. F. S. Andrade, and A. G. Brolo, "A review on the fabrication of substrates for surface enhanced Raman spectroscopy and their applications in analytical chemistry," *Analytica Chimica Acta*, vol. 693, no. 1-2, pp. 7–25, 2011.

[6] D.-Y. Wu, J.-F. Li, B. Ren, and Z.-Q. Tian, "Electrochemical surface-enhanced Raman spectroscopy of nanostructures," *Chemical Society Reviews*, vol. 37, no. 5, pp. 1025–1041, 2008.

[7] C. M. S. Izumi, G. F. S. Andrade, and M. L. A. Temperini, "Surface-enhanced resonance raman scattering of polyaniline on silver and gold colloids," *The Journal of Physical Chemistry B*, vol. 112, no. 51, pp. 16334–16340, 2008.

[8] J. C. Santos Costa, R. A. Ando, A. C. Sant'ana et al., "High performance gold nanorods and silver nanocubes in surface-enhanced Raman spectroscopy of pesticides," *Physical Chemistry Chemical Physics*, vol. 11, no. 34, pp. 7491–7498, 2009.

[9] J. Kneipp, H. Kneipp, and K. Kneipp, "SERS—a single-molecule and nanoscale tool for bioanalytics," *Chemical Society Reviews*, vol. 37, no. 5, pp. 1052–1060, 2008.

[10] S. E. J. Bell and N. M. S. Sirimuthu, "Quantitative surface-enhanced Raman spectroscopy," *Chemical Society Reviews*, vol. 37, no. 5, pp. 1012–1024, 2008.

[11] D. Graham and R. Goodacre, "Chemical and bioanalytical applications of surface enhanced Raman scattering spectroscopy," *Chemical Society Reviews*, vol. 37, no. 5, pp. 883–884, 2008.

[12] I. A. Larmour and D. Graham, "Surface enhanced optical spectroscopies for bioanalysis," *Analyst*, vol. 136, no. 19, pp. 3831–3853, 2011.

[13] D. A. Stuart, J. M. Yuen, N. Shah et al., "In vivo glucose measurement by surface-enhanced Raman spectroscopy," *Analytical Chemistry*, vol. 78, no. 20, pp. 7211–7215, 2006.

[14] B.-H. Jun, G. Kim, M. S. Noh et al., "Surface-enhanced Raman scattering-active nanostructures and strategies for bioassays," *Nanomedicine*, vol. 6, no. 8, pp. 1463–1480, 2011.

[15] A. C. Sant'Ana, T. C. R. Rocha, P. S. Santos, D. Zanchet, and M. L. A. Temperini, "Size-dependent SERS enhancement of colloidal silver nanoplates: the case of 2-amino-5-nitropyridine," *Journal of Raman Spectroscopy*, vol. 40, no. 2, pp. 183–190, 2009.

[16] J. Kneipp, H. Kneipp, W. L. Rice, and K. Kneipp, "Optical probes for biological applications based on surface-enhanced Raman scattering from indocyanine green on gold nanoparticles," *Analytical Chemistry*, vol. 77, no. 8, pp. 2381–2385, 2005.

[17] W. Leng, F. Würthner, and A. M. Kelley, "Resonance Raman intensity analysis of merocyanine dimers in solution," *The Journal of Physical Chemistry B*, vol. 108, no. 29, pp. 10284–10294, 2004.

[18] K. Kneipp, H. Kneipp, G. Deinum, I. Itzkan, R. R. Dasari, and M. S. Feld, "Single-molecule detection of a cyanine dye in silver colloidal solution using near-infrared surface-enhanced raman scattering," *Applied Spectroscopy*, vol. 52, no. 2, pp. 175–178, 1998.

[19] J. C. Rubim, M. L. A. Temperini, P. Corio et al., "Surface-enhanced raman spectroscopic (SERS and FT-SERS) investigation of the complex ion [Fe2(CN)10L]6- (L = 4,4′-bipyridine and pyrazine) adsorbed on silver and gold electrodes," *Journal of Physical Chemistry*, vol. 99, no. 1, pp. 345–355, 1995.

[20] D. F. de Carvalho, B. G. da Fonseca, I. L. Barbosa et al., "Surface-enhanced Raman scattering study of the redox adsorption of p-phenylenediamine on gold or copper surfaces," *Spectrochimica Acta Part A: Molecular and Biomolecular Spectroscopy*, vol. 103, pp. 108–113, 2013.

[21] E. C. Le Ru and P. G. Etchegoin, *Principles of Surface-Enhanced Raman Spectroscopy: And Related Plasmonic Effects*, Elsevier, Amsterdam, The Netherlands, 2009.

[22] M. M. Nobrega, K. S. Souza, G. F. S. Andrade, P. H. C. Camargo, and M. L. A. Temperini, "Emeraldine salt form of polyaniline as a probe molecule for surface enhanced raman scattering substrates excited at 1064 nm," *Journal of Physical Chemistry C*, vol. 117, no. 35, pp. 18199–18205, 2013.

[23] G. Frens, "Controlled nucleation for regulation of particle-size in monodisperse gold suspensions," *Nature Physical Science*, vol. 241, no. 105, pp. 20–22, 1973.

[24] P. C. Lee and D. Meisel, "Adsorption and surface-enhanced Raman of dyes on silver and gold sols," *The Journal of Physical Chemistry*, vol. 86, no. 17, pp. 3391–3395, 1982.

[25] K. Kneipp, Y. Wang, H. Kneipp et al., "Single molecule detection using surface-enhanced Raman scattering (SERS)," *Physical Review Letters*, vol. 78, no. 9, pp. 1667–1670, 1997.

[26] M. J. Frisch, G. W. Trucks, H. B. Schlegel et al., *Gaussian 09, Revision B.01*, Gaussian, Inc., Wallingford, Conn, USA, 2009.

[27] A. D. Becke, "Density-functional thermochemistry. III. The role of exact exchange," *The Journal of Chemical Physics*, vol. 98, no. 7, pp. 5648–5652, 1993.

[28] C. Lee, W. Yang, and R. G. Parr, "Development of the Colle-Salvetti correlation-energy formula into a functional of the electron density," *Physical Review B*, vol. 37, no. 2, pp. 785–789, 1988.

[29] B. Miehlich, A. Savin, H. Stoll, and H. Preuss, "Results obtained with the correlation energy density functionals of becke and Lee, Yang and Parr," *Chemical Physics Letters*, vol. 157, no. 3, pp. 200–206, 1989.

[30] A. D. McLean and G. S. Chandler, "Contracted Gaussian basis sets for molecular calculations. I. Second row atoms, Z=11–18," *The Journal of Chemical Physics*, vol. 72, no. 10, pp. 5639–5648, 1980.

[31] R. Krishnan, J. S. Binkley, R. Seeger, and J. A. Pople, "Self-consistent molecular-orbital methods. 20. Basis set for correlated wave-functions," *The Journal of Chemical Physics*, vol. 72, no. 1, pp. 650–654, 1980.

[32] W. B. Collier, I. Magdó, and T. D. Klots, "Infrared and Raman spectra of bicyclic molecules using scaled noncorrelated and correlated ab initio force fields," *Journal of Chemical Physics*, vol. 110, no. 12, pp. 5710–5720, 1999.

[33] R. Dennington, T. Keith, and J. Millam, *GaussView*, Version 3, Semichem, Shawnee Mission, Kan, USA, 2003.

[34] J. Fabian, H. Nakazumi, and M. Matsuoka, "Near-infrared absorbing dyes," *Chemical Reviews*, vol. 92, no. 6, pp. 1197–1226, 1992.

[35] A. Mishra, R. K. Behera, P. K. Behera, B. K. Mishra, and G. B. Behera, "Cyanines during the 1990s: a review," *Chemical Reviews*, vol. 100, no. 6, pp. 1973–2012, 2000.

[36] D. W. Mayo, F. A. Miller, and R. W. Hannah, *Course Notes on the Interpretation of Infrared and Raman Spectra*, John Wiley & Sons, Hoboken, NJ, USA, 2003.

[37] R. Aroca, *Surface-Enhanced Vibrational Spectroscopy*, John Wiley & Sons, New York, NY, USA, 2006.

[38] E. C. Le Ru, E. Blackie, M. Meyer, and P. G. Etchegoint, "Surface enhanced raman scattering enhancement factors: a comprehensive study," *Journal of Physical Chemistry C*, vol. 111, no. 37, pp. 13794–13803, 2007.

[39] D. C. Rodrigues, D. P. dos Santos, M. L. de Souza, G. F. S. Andrade, and M. L. A. Temperini, "Critical assessment of approaches for the calculation of enhancement factors in surface-enhanced Raman scattering for different substrates," submitted for publication.

[40] J. F. Padday, "Adsorption of cyanine dyes at silver-halide surfaces," *Transactions of the Faraday Society*, vol. 60, pp. 1325–1334, 1964.

[41] A. G. Brolo, D. E. Irish, and B. D. Smith, "Applications of surface enhanced Raman scattering to the study of metal-adsorbate interactions," *Journal of Molecular Structure*, vol. 405, no. 1, pp. 29–44, 1997.

[42] Z.-Q. Tian and B. Ren, "Adsorption and reaction at electrochemical interfaces as probed by surface-enhanced Raman spectroscopy," *Annual Review of Physical Chemistry*, vol. 55, pp. 197–229, 2004.